JVST A
Journal of Vacuum Science & Technology A

ARTICLE

avs.scitation.org/journal/jva

Thermal induced depletion of cationic vacancies in NiO thin films evidenced by x-ray absorption spectroscopy at the O 1s threshold

Cite as: J. Vac. Sci. Technol. A 38, 033209 (2020); doi: 10.1116/6.0000080
Submitted: 5 February 2020 · Accepted: 18 March 2020 ·
Published Online: 9 April 2020

Alejandro Gutiérrez,[1,a)] Guillermo Domínguez-Cañizares,[1] Stefan Krause,[2] Daniel Díaz-Fernández,[1] and Leonardo Soriano[1]

AFFILIATIONS

[1]Departamento de Física Aplicada and Instituto de Ciencia de Materiales Nicolás Cabrera, Universidad Autónoma de Madrid, Cantoblanco, 28049 Madrid, Spain
[2]Helmholtz-Zentrum Berlin für Materialien und Energie GmbH, Albert-Einstein-Straße 15, 12489 Berlin, Germany

[a)]**Electronic mail:** a.gutierrez@uam.es

ABSTRACT

The effects of thermal annealing on the concentration of cationic vacancies in p-type semiconducting NiO thin films have been studied by x-ray absorption spectroscopy at the O 1s threshold. This technique proves to be very sensitive to the amount of Ni vacancies through the intensity of a prepeak observed below the absorption threshold, associated with Ni ions in a high oxidation state. Samples with different vacancy concentrations were obtained by radio frequency magnetron sputtering with different O_2/Ar ratios in the plasma. Thermal effects have been studied both during thin film growth and after postprocessing annealing. In both cases, the observed effects were very similar, showing a depletion of cationic vacancies with temperature. By changing the surface sensibility of the x-ray absorption spectroscopy measurements, the authors could find out that the transition to stoichiometric NiO begins at the surface.

I. INTRODUCTION

The electrical properties of oxide materials are strongly influenced by the presence of vacancies and other point defects. While purely stoichiometric oxides are usually electrical insulators, vacancies can significantly increase their electrical conductivity, being n-type in the case of oxygen vacancies, as in ZnO,[1] or p-type in the case of cationic vacancies, as in NiO.[2] Many applications of these materials depend largely on their electrical conductivity, such as those related to chemical sensing, photovoltaics, energy storage and conversion, or photoelectronics.[3–5] Consequently, an understanding of the relationship between structure, defect concentration, and functional properties is essential to develop new applications. In the case of NiO, its p-character, and the possibility to tailor its properties by varying the processing parameters, make it a very interesting material in different fields.[6–10]

In previous works, we have investigated NiO thin films grown by magnetron sputtering from an NiO target using different O_2/Ar ratios in the plasma.[11–13] We found that the electrical conductivity of the films depends on the oxygen content in the plasma during growth, since it determines the amount of Ni vacancies in the NiO films.[11] Among other techniques, we used x-ray absorption spectroscopy (XAS) at the O 1s threshold as a reliable technique to obtain a direct measure of the density of vacancies in Ni defective NiO.[12] In this work, we show, using XAS at the O 1s threshold, that thermal annealing of NiO thin films with a certain vacancy concentration decreases this concentration down to doping levels. By varying the XAS probing depth, we were able to realize that the transition toward stoichiometric NiO begins at the surface. Two different types of experiments were carried out. A first set of samples was annealed at different temperatures during growth, and a second set was grown at room temperature and subsequently annealed during the XAS measurements. In both cases, the observed effects were very similar.

II. EXPERIMENT

NiO thin films were grown by RF magnetron sputtering from an NiO target (AJA International, 99.95% purity, 2 in. diameter)

on single-crystal silicon wafers [p-type with (100) orientation]. The deposition was performed in a high vacuum chamber with a base pressure in the range of 10^{-7} mbar. The pressure used for plasma ignition was 1.5×10^{-2} mbar and was maintained at this value during the whole growth process, which took approximately 1 h. The plasma was composed of a mixture of oxygen and argon, with an oxygen content ranging from 0% to 100%. The substrates were rotated during deposition at 10 rpm to obtain a more uniform film, without shaded areas. The angle of the sputtering cathode was 23° (off-axis) with respect to the normal of the substrate surface, and the distance between the target and the substrate was 8 cm. Before starting the deposition, a 5 min presputtering was performed to clean the target surface. The magnetron power was set at 200 W. The heating of the substrates during NiO growth was carried out by placing high-power halogen lamps just below the rotating sample holder. Samples were grown at three different substrate temperatures: without heating, at 200 °C, and at 300 °C. The temperature of the samples grown without heating gradually increased from room temperature to ~70 °C at the end of the deposition. This temperature rise was induced by the plasma. The temperature was measured on the surface of the substrates by an external IR pyrometer operating through a sapphire window. NiO films grown in this manner were polycrystalline, with thickness values between 100 and 240 nm, as determined with a Veeco Dektak 150+ Surface Profiler. The electrical resistivity of the films was measured at room temperature by the Van der Pauw method using an Ecopia HMS-5000 system.

O 1s x-ray absorption spectra were obtained at the Optics Beamline and the UE52-PGM Beamline of the BESSY II synchrotron radiation source. Most of the measurements were carried out in total electron yield mode (TEY), measuring the sample drain current. In addition, some samples were measured in total fluorescence yield mode (TFY), using a photodiode, to increase the probing depth. Note that TEY and TFY have different probing depths, the latter being more bulk sensitive. The photon energy was calibrated by comparing the binding energy of the Au $4f_{7/2}$ photoemission peak excited with first-order and second-order light. The energy resolution was approximately 100 meV at a photon energy of about 500 eV. The spectra were recorded at normal incidence and normalized using a spectrum from a fresh gold sample to correct the spectra for the contamination of the optical elements and other possible artifacts. Some samples were annealed *in situ* during XAS measurements. The sample holder of the UHV system was equipped with a heater located below the sample to reach high temperatures, which were measured using a thermocouple.

III. RESULTS AND DISCUSSION

Figure 1 shows x-ray absorption spectra at the O 1s threshold, taken in TEY mode, of NiO thin films grown at different

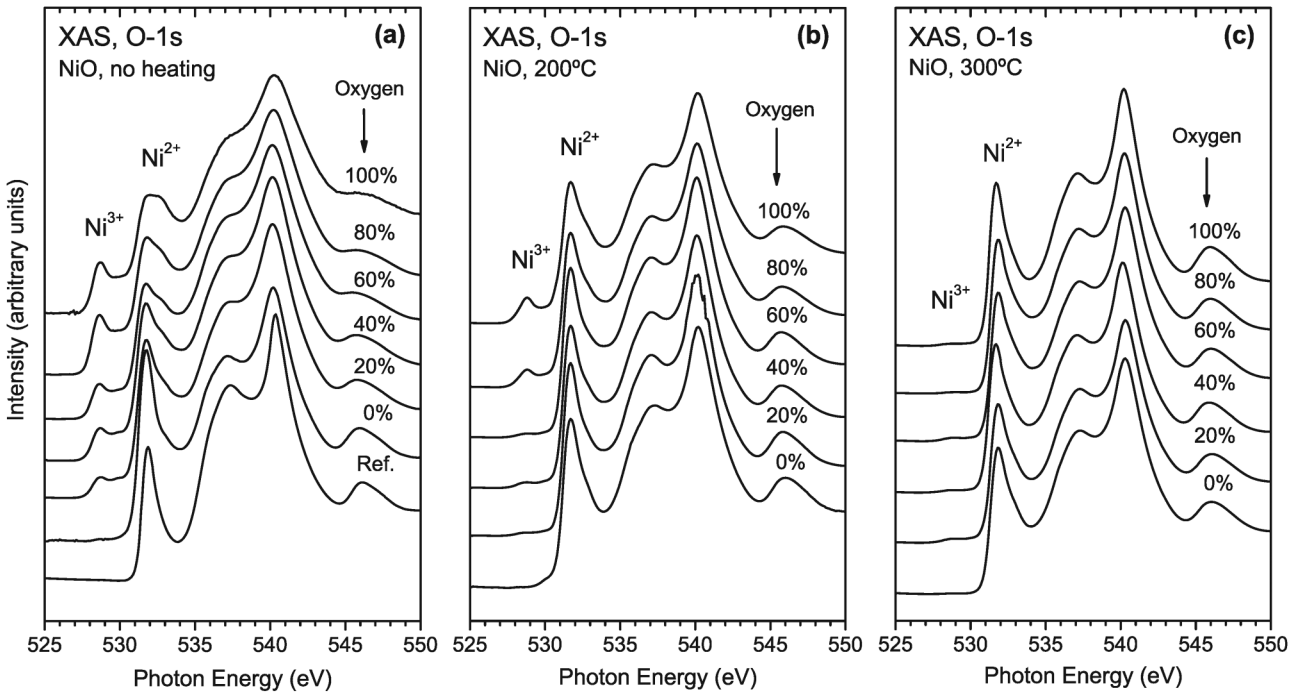

FIG. 1. X-ray absorption spectra at the O 1s threshold, taken in TEY mode, of NiO thin films grown without heating the substrate (a), and after heating the substrate at 200 °C (b) and at 300 °C (c). In each case, the oxygen/argon ratio in the sputtering plasma varied between 0% and 100%, as indicated in the right part of the figures. The spectrum labeled "Ref." in (a) corresponds to a reference polycrystalline NiO sample. The "Ni^{2+}" and "Ni^{3+}" labels identify features in the spectra associated with Ni ions in different environments (see text).

temperatures and with different oxygen contents in the plasma. O 1s XAS spectra reveal transitions to unoccupied O p states in the conduction band. However, in the case of transition metal oxides, the spectra reflect, through the corresponding metal-oxygen hybridization, information on the unoccupied metal 3d band.[14] Figure 1(a) shows a series of spectra of samples grown without heating and with different oxygen contents in the plasma. In addition, a spectrum obtained on a reference polycrystalline NiO sample, labeled "Ref.," is included at the bottom. The first peak in this reference spectrum, at ~532 eV, is assigned to unoccupied Ni e_g states. The structures at higher energies, at 537.5 and 540.5 eV, respectively, correspond to O 2p states mixed with Ni 4sp states.[15] The first spectrum of the series, grown without oxygen (0%), is very similar to the spectrum of the reference NiO sample, confirming that this sample can be assigned to polycrystalline NiO.

As the oxygen content of the plasma increases, several changes in the XAS spectra are observed. In addition to a general broadening, the peak at 532 eV splits into two components due to a reduction in the symmetry induced by surface effects. This is because the addition of oxygen causes a refinement of the crystal size in the polycrystalline NiO thin films.[12,13] This refinement could also be the reason for the general broadening of the spectra. On the other hand, a new peak appears at 529 eV and its intensity increases with the oxygen content in the plasma. This new peak is assigned to O 2p states mixed with Ni^{3+} 3d states and, therefore, can be associated with Ni vacancies.[12] The intensity of this peak is approximately proportional to the oxygen content of the plasma during growth.[12] The presence of nickel oxide phases other than NiO can be ruled out in view of previous results obtained using Ni 2p edge XAS and x-ray diffraction.[11,12] These previous results are consistent with the spectra shown in Fig. 1.

Figure 1(b) shows a similar series of XAS spectra but for samples grown at 200 °C. In this case, both effects, the surface induced splitting and the presence of the prepeak, are much less evident than for samples grown without heating. In fact, only samples grown with 80% and 100% oxygen content in the plasma show significant prepeak intensity, being barely noticeable for samples grown with lower oxygen content, and nonexistent for the sample grown without oxygen. The effect is even more evident in Fig. 1(c), where XAS spectra for samples grown at 300 °C are shown. In this case, the prepeak intensity is barely noticeable for any oxygen content in the plasma and again nonexistent for the sample grown without oxygen.

By adding oxygen to the plasma during growth, part of this oxygen incorporates into the NiO films, leading to the creation of Ni vacancies. These nickel vacancies, created at cation sites, modify the local environment around the surrounding Ni ions, promoting ionization of some Ni^{2+} ions to Ni^{3+} ions without changing the NiO crystal structure.[11] This ionization gives rise to the prepeak observed in Fig. 1.[12] However, according to the results shown in Figs. 1(b) and 1(c), the amount of excess oxygen depends on the substrate temperature during growth. Since Ni^{3+} ions are less stable than Ni^{2+} ions, a thermodynamical trend is expected to reduce the oxygen excess. This process must be promoted by diffusion, and, consequently, thermally activated. However, the thermal energy available at room temperature does not seem sufficient to evacuate the excess oxygen as it is incorporated into the NiO lattice. An increase in the substrate temperature to 300 °C provides enough thermal energy to drain the excess oxygen as it reaches the film. In any case, the intensity of the prepeak does not disappear completely, suggesting that NiO obtained retains a small amount of cationic vacancies and, therefore, its p-character. Similar results have been obtained using different NiO synthesis methods.[16]

Figure 2 shows more clearly the differences observed in the XAS spectra of samples grown under different conditions. This figure shows XAS spectra at the O 1s threshold of samples grown with the two extreme oxygen contents (0% and 100%) and for the three different temperatures used in this work: RT for the curves at

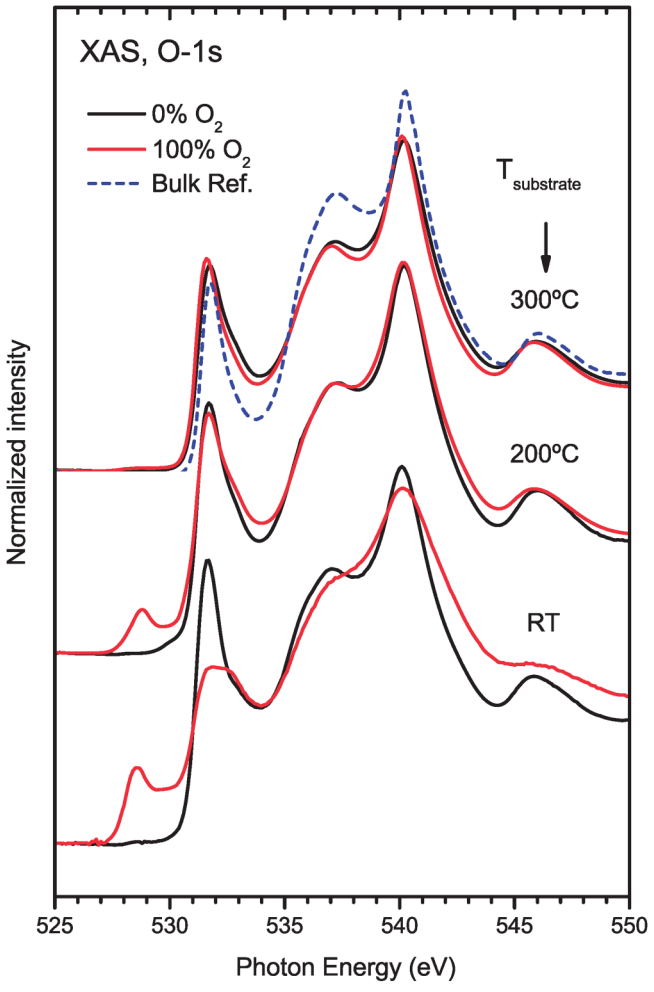

FIG. 2. X-ray absorption spectra at the O 1s threshold, taken in the TEY mode, of NiO samples grown with the two extreme oxygen contents (0%, black line and 100%, red line), and at the three temperatures used in this work: RT for the curves at the bottom, 200 °C for the curves in the middle, and 300 °C for the curves at the top. The intensities have been rescaled to compare spectra with different oxygen contents. The dashed spectrum shown at the top of the figure corresponds to a reference polycrystalline NiO sample.

the bottom, 200 °C for the curves in the middle, and 300 °C for the curves at the top. The intensities have been rescaled in order to compare spectra with different oxygen contents. The effect of the temperature is now easily observed: as the substrate temperature increases, the main features of the XAS spectra converge to those of the NiO bulk reference, represented as a dashed line at the top of the figure. At 300 °C, the pre-edge peak almost disappears, although a residual intensity can still be observed. This persistence of the prepeak upon annealing suggests that a small amount of Ni^{3+} vacancies remains and would eventually require higher temperatures to be completely removed. On the other hand, the splitting of the peak at 532 eV is also greatly affected by the increase in temperature: at 200 °C it is barely observed, less for the sample grown with pure oxygen. In any case, remanent surface effects are present even at 300 °C, as suggested by the differences observed between thin films and bulk NiO spectra in the top graphs. Even at this temperature, the nanostructured morphology of the films with respect to bulk NiO can explain the general broadening observed in the spectra.[13]

As mentioned above, the electrical conductivity of NiO strongly depends on the concentration of Ni vacancies.[11,17] According to Figs. 1 and 2, the lower the temperature during growth and the higher the oxygen content in the plasma, the larger the density of vacancies. Consequently, the resistivity is expected to be higher for samples grown with lower oxygen content and higher temperatures. This trend can be observed in Fig. 3, where the electrical resistivity is shown in terms of both parameters: substrate temperature and oxygen content in the plasma. Despite some dispersion, the general trend is as expected: the curve corresponding to samples grown at 200 °C is, in general, below that of samples grown at 300 °C and above that of samples grown at room temperature. For each series, the trend is mostly decreasing with the increase in plasma oxygen content. The observed dispersion and deviations from the trend can be due to inhomogeneities in composition and thickness in the samples. It is interesting to note that the largest measured resistivity value, at 0% oxygen content, is below 1 kΩ cm, a value several orders of magnitude lower than the one expected for purely stoichiometric NiO,[18] which suggests that some level of Ni vacancies remains even for the sample grown without oxygen at the highest temperature used in this work. This is probably related to the residual presence of the prepeak observed in Figs. 1 and 2 for samples grown at high temperatures and low oxygen content, compared to the reference polycrystalline NiO sample, where no traces of the prepeak are observed.

So far, we have focused on the effects of substrate heating during growth. Figure 4 shows that similar effects are found after postprocessing sample annealing under ultrahigh vacuum (UHV)

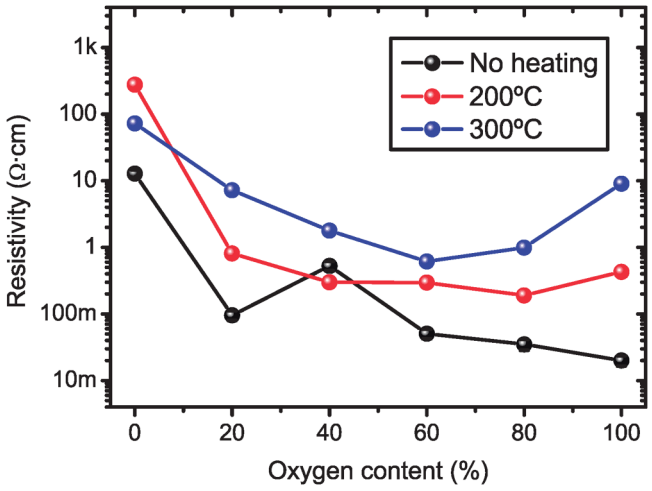

FIG. 3. Electrical resistivity as a function of the oxygen content in the plasma for samples grown at different substrate temperatures. The lines in the graph connect data points for samples grown at the same temperature.

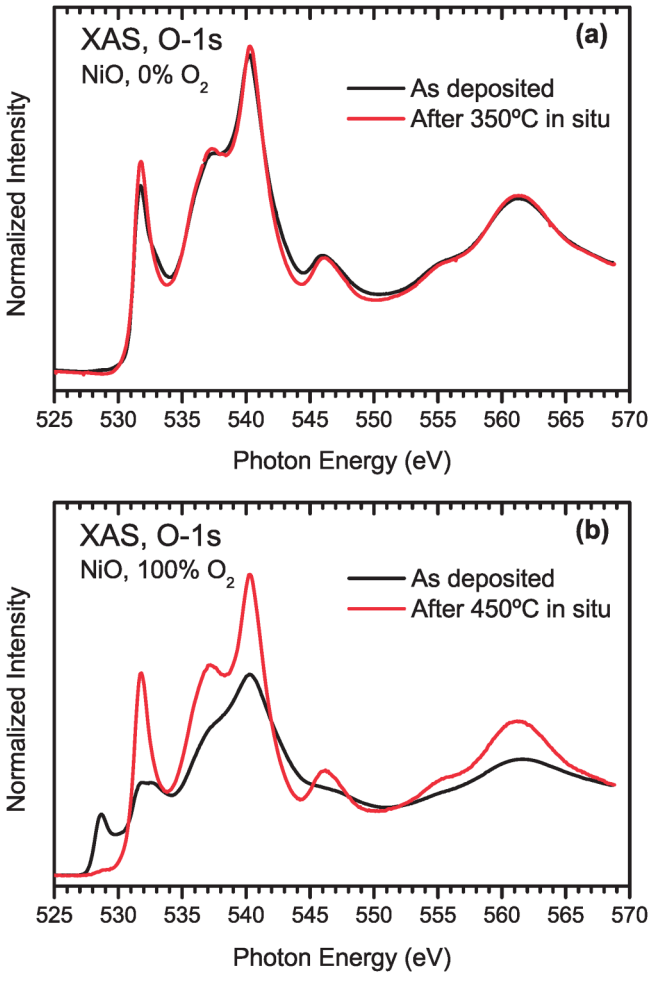

FIG. 4. X-ray absorption spectra at the O 1s threshold, taken in the TEY mode, of NiO films grown (a) with 0% oxygen and (b) with 100% oxygen in the plasma. The black line represents the spectra of films as-deposited at RT, before thermal treatment is applied, and the red curve corresponds to the spectra after *in situ* annealing at 350 °C (a) and 450 °C (b) in UHV, respectively.

conditions. Figure 4(a) shows XAS spectra of NiO films grown without oxygen at RT. The black line represents the spectrum of the film as-deposited, before applying the heat treatment. The red curve (color in the online version) corresponds to the spectrum after annealing *in situ* at 350 °C in UHV. Although weak, the effect of the annealing is evident: the peaks corresponding to hybridized Ni–O states become narrower, and the shoulder at 533 eV, assigned to surface effects, disappears. The effects of annealing are much more evident for NiO films grown with the pure oxygen plasma, as shown in Fig. 4(b). The black curve corresponds to the NiO film grown at RT and the red curve to the same sample after annealing at 450 °C in UHV. As can be seen in the figure, the XAS spectrum undergoes substantial changes after this thermal treatment: the pre-edge peak due to Ni^{3+} ions, as well as the shoulder due to the 3d e_g sub-band splitting, disappear. Final states located at higher energies, above 535 eV, increase their intensity and become narrower, resembling a more ordered crystal structure, with larger crystallite size, where the lifetime of the excited states is longer. It should be noted here that both red curves, corresponding to different samples after the annealing process, are very similar to each other. This fact suggests a convergence toward a nickel oxide structure with similar stoichiometry and long-range order.

The changes described above upon *in situ* thermal treatment are expected to take place gradually. Figure 5 shows XAS spectra, obtained in the TEY mode at the region near the oxygen 1s absorption edge, of samples grown with different plasma oxygen contents, taken at different temperatures. The spectra show the region of the pre-edge peak, at ~528.7 eV, and the main peak, corresponding to Ni^{2+} e_g states, at ~532 eV. For each sample, several spectra were obtained while heating the sample. The different colors of the spectra shown in Fig. 5 correspond to different sample temperatures during measurement. The XAS spectrum of the sample grown in pure Argon (0%) is not shown due to the absence of prepeak for this sample. It is evident from a direct inspection of the figure that a gradual increase in temperature produces a gradual decrease in the intensity of the pre-edge peak, as well as a reduction of the splitting of the Ni^{2+} e_g states and a narrowing of the main peak. For each sample, the temperature was gradually increased until the intensity of the prepeak became negligible. It is interesting to note that the higher the oxygen content in the plasma, the

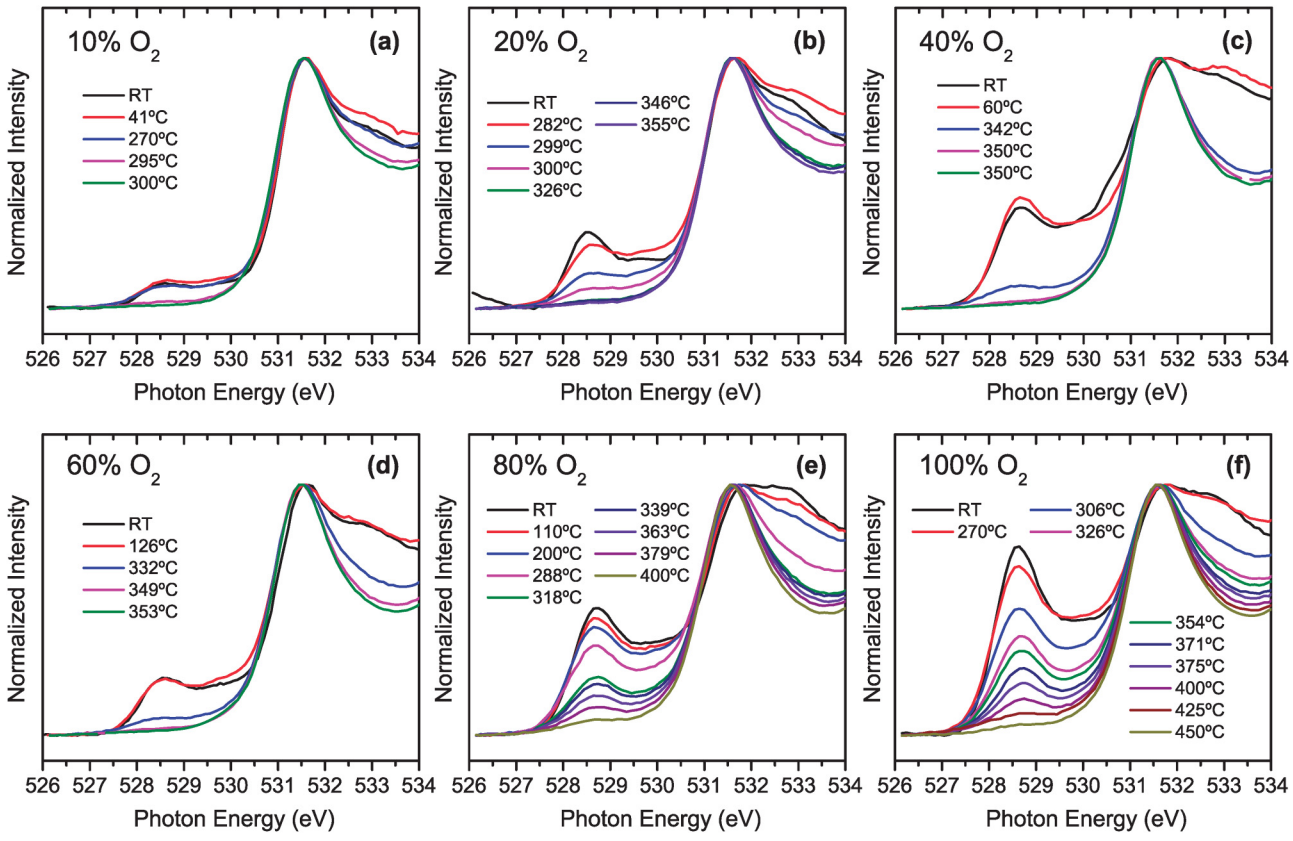

FIG. 5. X-ray absorption spectra at the region near the oxygen 1s absorption threshold, taken in the TEY mode, of NiO samples grown with different oxygen contents in the plasma, from 10% to 100%, taken at different temperatures, as indicated by the different colors of the spectra. The general trend shows a decrease in the intensity of the pre-edge peak upon annealing. The highest temperature shown in the figure is different for each sample, corresponding to the temperature at which the intensity of the prepeak is negligible.

higher the final temperature needed to make the pre-edge peak intensity close to zero. This final temperature varies from ~300 °C for the sample grown with 10% oxygen in the plasma to ~450 °C for the sample grown with pure oxygen.

This increase in the final temperature at which the Ni^{3+} related peak disappears with the oxygen content can be seen more clearly in Fig. 6. This figure shows the temperature at which the pre-edge peak decreases below a 5% of the initial intensity as a function of the oxygen content in the sputtering plasma. This temperature increases from 300 °C for the sample grown with 10% oxygen in the plasma to 450 °C for the sample grown with pure oxygen. There is, therefore, a clear correlation between the intensity of the prepeak in the as-grown state and the temperature needed to remove it upon annealing. The addition of oxygen to the sputtering plasma creates a certain amount of Ni vacancies within the NiO lattice, as evidenced by the presence of the prepeak in the XAS spectra. The amount of such vacancies increases with the oxygen content in the plasma, but the presence of these ionic defects presumably causes some lattice disorder and internal stress. The annealing of the thin films has a healing effect that brings the system into a more ordered state in which the number of point defects decreases. Figure 6 shows that the larger the amount of Ni vacancies initially introduced into the NiO lattice, the larger the thermal energy necessary to remove them.

As it is well established, the information obtained by XAS in TEY mode is limited to a few nanometers below the surface of the sample, i.e., it is considered a surface sensitive technique.[19,20] On the other hand, the probing depth of XAS in TFY varies between several tens and a few hundred nanometers, depending on the photon energy. In addition to the TEY results shown so far, we performed XAS measurements in TFY mode of some samples after annealing. Figure 7 shows the prepeak region of samples grown with 20%, 40%, and 80% oxygen after annealing was completed, that is, after the prepeak had disappeared from the spectra obtained in the TEY mode. Both TEY spectra (black) and TFY spectra (red in the online version) are shown for each sample. As can be seen, the prepeak is still visible in the spectra obtained in TFY mode (red line) on samples grown with 40% and 80% oxygen in the plasma, and the broadening of the main peak remains for all samples. In any case, the intensity of the prepeak is reduced as compared to the initial intensity [see Fig. 1(a)].

Annealing supplies additional energy to the system and allows a diffusion driven ordering of the crystalline structure, recovering stoichiometry, and reducing Ni^{3+} impurities. In this process, the excess oxygen in the lattice escapes the samples after crossing the surface. Consequently, there seems to be a depletion zone near the surface where the amount of defects is lower. This is supported by the absence of the prepeak in the TEY spectra for annealed samples. However, the prepeak is still visible in the TFY spectra because, below this surface region, the system has not yet recovered

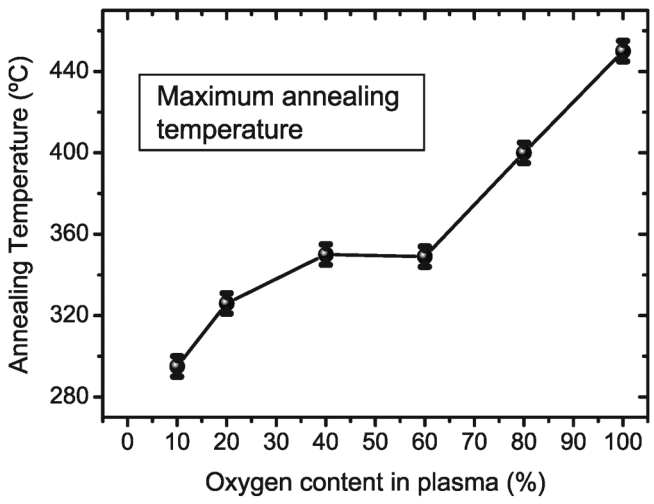

FIG. 6. Maximum annealing temperature used during the x-ray absorption measurements shown in Fig. 5, as a function of the oxygen content in the sputtering plasma. This maximum temperature is determined as the temperature that produces a decrease in the pre-edge peak intensity below 5% of the initial intensity.

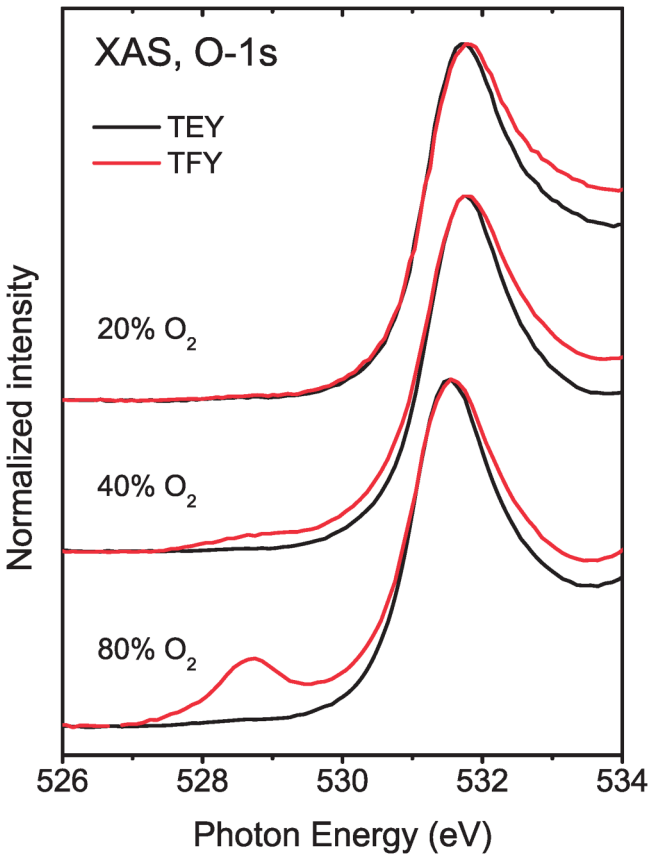

FIG. 7. X-ray absorption spectra at the region near the oxygen 1s absorption threshold, taken in the TEY detection mode (black lines) and TFY detection mode (red lines), of NiO samples grown with 20%, 40%, and 80% oxygen in the plasma after annealing.

the equilibrium situation. Much higher temperature and longer times would be needed to irreversibly reduce the prepeak in the bulk. When the thin film loses its excess oxygen and recovers the stoichiometry, its behavior resembles that of the NiO reference in terms of XAS signals.

IV. CONCLUSIONS

We have investigated the effect of annealing on the concentration of vacancies in p-doped NiO thin films by x-ray absorption spectroscopy at the O 1s threshold. NiO samples with different concentrations of vacancies were grown by magnetron sputtering with variable oxygen content in the plasma. The number of vacancies in NiO films is directly related to the intensity of a prepeak that appears at 529 eV, below the O absorption threshold in the XAS spectra. The annealing of the substrates during growth produces a clear decrease in the density of vacancies and, consequently, in the concentration of Ni^{3+} ions, as evidenced by the decrease in prepeak intensity in the XAS spectra taken in the TEY mode. The rest of the structures observed in the XAS spectra show a refinement upon annealing that can be associated with better crystallinity. We have also studied the effect of postprocessing annealing. The results show a decrease in the vacancy concentration with the temperature. The temperature at which the prepeak disappears in the XAS spectra obtained in TEY mode increases with the plasma oxygen content during NiO growth. On the other hand, the TFY measurements reveal that, after reaching this final temperature, the prepeak is still visible. Given the larger probing depth of XAS in TFY mode, this indicates that the dynamics of vacancy recombination takes places at the surface and progresses toward the inner part of the samples.

ACKNOWLEDGMENTS

This work was partially supported by the Spanish MICINN, under Project No. ENE2010-21198-C04-04 and by the Comunidad de Madrid under Project No. NANOMAGCOSTCM-P2018/NMT4321. The authors acknowledge the Helmholtz-Zentrum Berlin for provision of synchrotron radiation beamtime at the Optics beamline and at the UE52-PGM beamline of BESSY II. Technical assistance during XAS measurements from R. Ovsyannikov is also acknowledged. The research leading to these results has received funding from the European Community's Seventh Framework Programme (FP7/2007–2013) under Grant Agreement No. 312284.

REFERENCES

[1]L. Liu, Z. Mei, A. Tang, A. Azarov, A. Kuznetsov, Q.-K. Xue, X. Du, Phys. Rev. B **93**, 235305 (2016).
[2]W.-L. Jang, Y.-M. Lu, W.-S. Hwang, T.-L. Hsiung, and H. P. Wang, Appl. Phys. Lett. **94**, 062103 (2009).
[3]M. Lorenz *et al.*, J. Phys. D Appl. Phys. **49**, 433001 (2016).
[4]A. Mirzaei and G. Neri, Sens. Actuators B **237**, 749 (2016).
[5]Y. Ren, Z. Ma, and P. G. Bruce, Chem. Soc. Rev. **41**, 4909 (2012).
[6]S. Yamada, T. Yoshioka, M. Miyashita, K. Urabe, and M. Kitao, J. Appl. Phys. **63**, 2116 (1988).
[7]K. Arora, M. Tomar, and V. Gupta, Biosens. Bioelectron. **30**, 333 (2011).
[8]M. D. Irwin, B. Buchholz, A. W. Hains, R. P. H. Chang, and T. J. Marks, Proc. Natl. Acad. Sci. U.S.A. **105**, 2783 (2008).
[9]K. C. Liu and M. A. Anderson, J. Electrochem. Soc. **143**, 124 (1996).
[10]H.-L. Chang, T. C. Lu, H. C. Kuo, and S. C. Wang, J. Appl. Phys. **100**, 124503 (2006).
[11]A. Gutiérrez, G. Domínguez-Cañizares, J. A. Jimenez, I. Preda, D. Díaz-Fernández, F. Jiménez-Villacorta, G. R. Castro, J. Chaboy, and L. Soriano, Appl. Surf. Sci. **276**, 832 (2013).
[12]R. J. O. Mossanek, G. Domínguez-Cañizares, A. Gutiérrez, M. Abbate, D. Díaz-Fernández, and L. Soriano, J. Phys. Condens. Mater. **25**, 495506 (2013).
[13]G. Domínguez-Cañizares, A. Gutiérrez, J. Chaboy, D. Díaz-Fernández, G. R. Castro, and L. Soriano, J. Mater. Sci. **49**, 2773 (2014).
[14]F. De Groot, M. Grioni, J. C. Fuggle, J. Ghijsen, G. A. Sawatzky, and H. Petersen, Phys. Rev. B **40**, 5715 (1989).
[15]L. Soriano, A. Gutiérrez, I. Preda, S. Palacin, J. M. Sanz, M. Abbate, J. F. Trigo, A. Vollmer, and P. R. Bressler, Phys. Rev. B **74**, 193402 (2006).
[16]P. Dubey and N. Kaurav, J. Phys. Conf. Ser. **836**, 012040 (2017).
[17]D. Soo Kim and H. Chul Lee, J. Appl. Phys. **112**, 034504 (2012).
[18]D. Adler and J. Feinleib, Phys. Rev. B **2**, 3112 (1970).
[19]M. Abbate, J. B. Goedkoop, F. De Groot, M. Grioni, J. C. Fuggle, S. Hofmann, H. Petersen, and M. Sacchi, Surf. Interface Anal. **18**, 65 (1992).
[20]B. H. Frazer, B. Gilbert, B. R. Sonderegger, and G. De Stasio, Surf. Sci. **537**, 161 (2003).